LDA+DMFT spectral functions and effective electron mass enhancement in the superconductor LaFePO

S. L. Skornyakov,[1,2] N. A. Skorikov,[1] A. V. Lukoyanov,[1,2] A. O. Shorikov,[1,2] and V. I. Anisimov[1,2]

[1]*Institute of Metal Physics, Russian Academy of Sciences, 620990 Ekaterinburg, Russia*

[2]*Ural State Technical University, 620002 Ekaterinburg, Russia*

In this paper we report LDA+DMFT results (method combining local-density approximation with dynamical mean-field theory) for spectral properties of superconductor LaFePO. Calculated **k**-resolved spectral functions reproduce recent angle-resolved photoemission spectroscopy data [D. H. Lu *et al.*, Nature (London) **455**, 81 (2008)]. Obtained effective electron mass enhancement values $m^*/m \approx 1.9-2.2$ are in good agreement with infrared and optical studies [M. M. Qazilbash *et al.*, Nat. Phys. **5**, 647 (2009)], de Haas–van Alphen, electrical resistivity, and electronic specific-heat measurements results that unambiguously evidence for moderate correlations strength in LaFePO. Similar values of m^*/m were found in the other Fe-based superconductors with substantially different superconducting transition temperatures. Thus, the dynamical correlation effects are essential in the Fe-based superconductors, but the strength of electronic correlations does not determine the value of superconducting transition temperature.

I. INTRODUCTION

The discovery of superconductivity with the transition temperature $T_c \approx$ 4 K in LaFePO (Ref. 1) and $T_c \approx 26-55$ K in $R\mathrm{O}_{1-x}\mathrm{F}_x\mathrm{FeAs}$ ($R=$La,Sm) (Ref. 2) has generated great interest to the new class of Fe-based superconductors.[3] While the microscopic mechanism of superconductivity in LaFePO is not yet clear,[4,5] its electronic properties have been studied extensively. Various experiments revealed the presence of electronic correlations in LaFePO. Analyzing angle-resolved photoemission spectroscopy (ARPES) data, Lu *et al.*[6] demonstrated that the density-functional theory (DFT) band structure should be renormalized by a factor of 2.2 to fit the experimental angle-resolved photoemission spectra. From infrared and optical conductivity data, the authors of Ref. 7 made a conclusion that the effective electron mass renormalization is about 2 in LaFePO. Similarly, the electron mass renormalization obtained from de Haas–van Alphen study is $m^*/m \approx 1.7-2.1$ (Ref. 8). Comparison of the experimental electronic specific-heat coefficient $\gamma_n = 10.1$ mJ/mol K^2 for LaFePO (Ref. 9) with the DFT value 5.9 mJ/mol K^2 (Ref. 10) gives the value of 1.7 for electron mass enhancement. Also the electrical resistivity at low temperatures has T^2 dependence[5,9] showing importance of correlation effects. However, the authors of Ref. 11 from analysis of x-ray absorption spectroscopy (XAS) and resonant inelastic x-ray scattering (RIXS) data for several iron pnictide compounds ($\mathrm{SmO}_{0.85}\mathrm{FeAs}, \mathrm{BaFe}_2\mathrm{As}_2, \mathrm{LaFe}_2\mathrm{P}_2$) arrived at a conclusion that correlations are not very strong here.

So far only a few electronic structure calculations for LaFePO by the DFT-based first-principles methods without any account for electronic correlations have been reported[6,10,12–14] thus making the problem of correlation effects study for this material very timely.

The combination of DFT and dynamical mean-field theory (DMFT) called LDA+DMFT method[15] is presently recognized state-of-the-art many-particle method to study correlation effects in real compounds. LDA+DMFT calculations for the FeAs-based superconductors[16–19] lead to diverse conclusions on the strength of electron correlations in these materials. The authors of Ref. 19 have proposed an extended classification scheme of the electronic correlation strength in the Fe pnictides based on analysis of several relevant quantities: a ratio of the Coulomb parameter U and the band width $W(U/W)$, quasiparticle mass enhancement m^*/m, **k**-resolved and **k**-integrated spectral functions $A(\mathbf{k}, \omega)$ and $A(\omega)$. Applying this scheme to LDA+DMFT results for $\mathrm{BaFe}_2\mathrm{As}_2$ they came to conclusion that this material should be regarded as a *moderately* correlated metal. In this work we report the results of LDA+DMFT study for electronic correlation effects in LaFePO. For this purpose we have calculated spectral functions $A(\mathbf{k}, \omega)$, effective electron mass enhancement m^*/m and compare our results with the available measurements for LaFePO finding very good agreement between calculated and experimental data. A moderate spectral functions renormalization corresponding to $m^*/m \approx 2$ was found in LaFePO similar to values obtained for $\mathrm{BaFe}_2\mathrm{As}_2$ (Ref. 19) while superconducting transition temperature in those materials could be an order of magnitude different.

II. METHOD

The LDA+DMFT scheme is constructed in the following way: first, a Hamiltonian $\hat{H}_{\mathrm{LDA}}$ is produced using converged LDA results for the system under investigation, then the many-body Hamiltonian is set up, and finally the corresponding self-consistent DMFT equations are solved. By projecting onto Wannier functions,[20] we obtain an effective 22-band Hamiltonian which incorporates five Fe d, three O p, and three P p orbitals per formula unit. In the present study we construct Wannier states for an energy window including both p and d bands. Thereby hybridization effects between p and d electrons were explicitly taken into account and eigen-

values of the Wannier functions Hamiltonian $\hat{H}_{LDA}$ exactly correspond to the 22 Fe, O, and P bands from LDA. The LDA calculations were performed with the experimentally determined crystal structure[21] using the Elk full-potential linearized augmented plane-wave (FP-LAPW) code.[22] Parameters controlling the LAPW basis were kept to their default values. The calculated LDA band structure $\epsilon_{LDA}(\mathbf{k})$ was found to be in good agreement with that of Lebègue *et al.* (Ref. [10]).

The many-body Hamiltonian to be solved by DMFT has the form

$$\hat{H} = \hat{H}_{LDA} - \hat{H}_{dc} + \frac{1}{2} \sum_{i,\alpha,\beta,\sigma,\sigma'} U_{\alpha\beta}^{\sigma\sigma'} \hat{n}_{i\alpha\sigma}^d \hat{n}_{i\beta\sigma'}^d, \quad (1)$$

where $U_{\alpha\beta}^{\sigma\sigma'}$ is the Coulomb interaction matrix, $\hat{n}_{i\alpha\sigma}^d$ is the occupation number operator for the d electron with orbital α or β and spin indices σ or σ' in the ith site. The term $\hat{H}_{dc}$ stands for the d-d interaction already accounted in LDA, so-called double-counting correction. The double counting has the form $\hat{H}_{dc} = \bar{U}(n_{DMFT} - \frac{1}{2})\hat{I}$, where n_{DMFT} is the total self-consistent number of d electrons obtained within the LDA+DMFT and $\bar{U}$ is the average Coulomb parameter for the d shell.

The DMFT self-consistency equations were solved iteratively for imaginary Matsubara frequencies. The auxiliary impurity problem was solved by the hybridization function expansion continuous-time quantum Monte Carlo (CTQMC) method.[23] In the present implementation of the CTQMC impurity solver the Coulomb interaction is taken into account in density-density form. The elements of $U_{\alpha\beta}^{\sigma\sigma'}$ matrix were parameterized by U and J according to procedure described in Ref. [24]. We used interaction parameters $\bar{U}$ = 3.1 eV and J = 1 eV similar to the values calculated by the constrained LDA method for Wannier functions[25] in Fe pnictides.[18] Calculations were performed in the paramagnetic state at the inverse temperature $\beta = 1/T = 20$ eV^{-1}. The real-axis self-energy needed to calculate spectral functions was obtained by the Padé approximant[26] (see the Appendix).

III. RESULTS AND DISCUSSION

The orbitally resolved Fe $3d$, O p, and P p spectral functions computed within LDA and LDA+DMFT, respectively, are compared in Fig. 1. Within the LDA all five Fe d orbitals form a common band in the energy range $(-2.5, +2.0)$ eV relative to the Fermi level (band width $W \approx 4.5$ eV). There is a significant hybridization of the Fe d orbitals with the P p and O p orbitals, leading to appearance of Fe d states contribution in the energy interval $(-5.5, -2.5)$ eV where the P p band is located. The corresponding features of LDA+DMFT spectral functions (upper panel in Fig. 1) in the energy area $(-5.5, -2.5)$ eV should not be mistaken for Hubbard bands because the same peaks are present in noncorrelated LDA bands (lower panel in Fig. 1). Correlation effects do not result in Hubbard bands appearance but lead to significant renormalization of the spectral function around the Fermi energy: "compressing" of energy scale so that separation between peaks of LDA+DMFT curves becomes ≈ 2
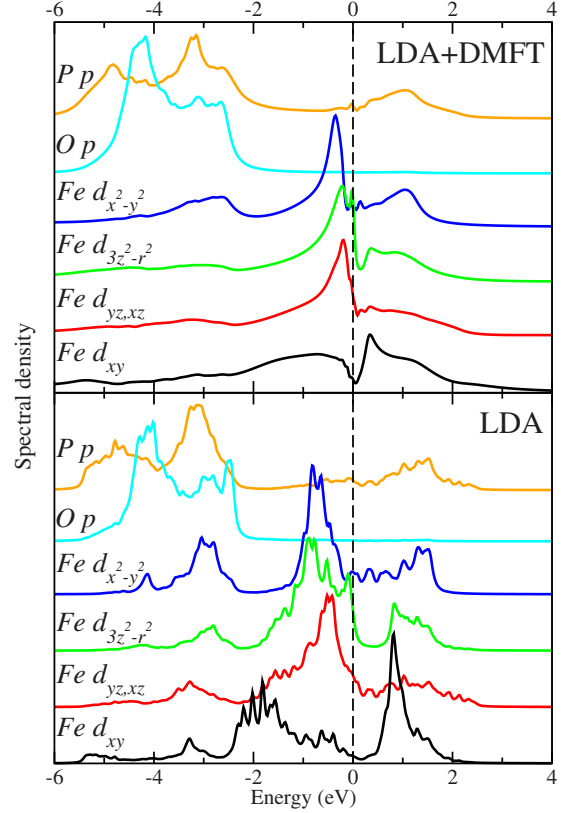

FIG. 1. (Color online) Orbitally resolved Fe $3d$, O p, and P p normalized spectral functions of LaFePO obtained within LDA+DMFT (upper panel) are compared with the LDA results (lower panel).

times smaller than in corresponding noncorrelated spectra.

It is instructive to plot energy dependence of real part of self-energy Re $\Sigma(\omega)$ (see Fig. 2). Peaks in spectral function $A(\mathbf{k}, \omega)$ are determined by the poles of $[\omega - \epsilon(\mathbf{k}) - \Sigma(\omega)]^{-1}$ function or the energy values $\omega = \epsilon(\mathbf{k}) + $ Re $\Sigma(\omega)$ [here $\epsilon(\mathbf{k})$ is noncorrelated band dispersion]. In Fig. 2 together with Re $\Sigma(\omega)$ a function $\omega + (H_{dc})_{ii}$ is plotted as a stripe having the width of noncorrelated band $\epsilon(\mathbf{k})$. The peaks of spectral function $A(\mathbf{k}, \omega)$ correspond to energy area where this stripe crosses Re $\Sigma(\omega)$ curve. As one can see such crossing happens only once in the energy interval around the Fermi level so that spectral functions will have only poles corresponding to quasiparticle bands and no Hubbard band poles will be observed.

A quantitative measure of the electron correlation strength is provided by the quasiparticle renormalization factor $Z = (1 - \frac{\partial \Sigma}{\partial \omega}|_{\omega=0})^{-1}$ which gives an effective mass enhancement $m^*/m = Z^{-1}$. In general, the self-energy is a matrix, leading to different effective masses for different bands. The calculated m^*/m values for every d-orbital are presented in Table I. The $d_{x^2-y^2}$ orbital has the smallest effective mass renormalization $m^*/m = 1.942$. The other d orbitals have approximately the same value $m^*/m \approx 2.2$.

The calculated effective mass enhancement $m^*/m \approx 1.9-2.2$ in LaFePO agrees very well with the de Haas–van Alphen experiments[8] where it was found to range from 1.7 to 2.1, and with the estimations of the effective
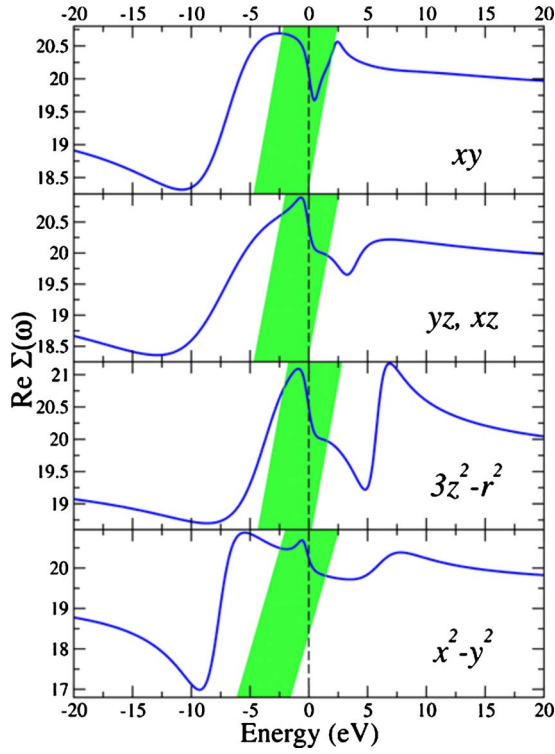
FIG. 2. (Color online) The real part of the self-energy $\Sigma(\omega)$ (black line) depicted together with $\omega + (H_{dc})_{ii}$ (light stripe, see text).
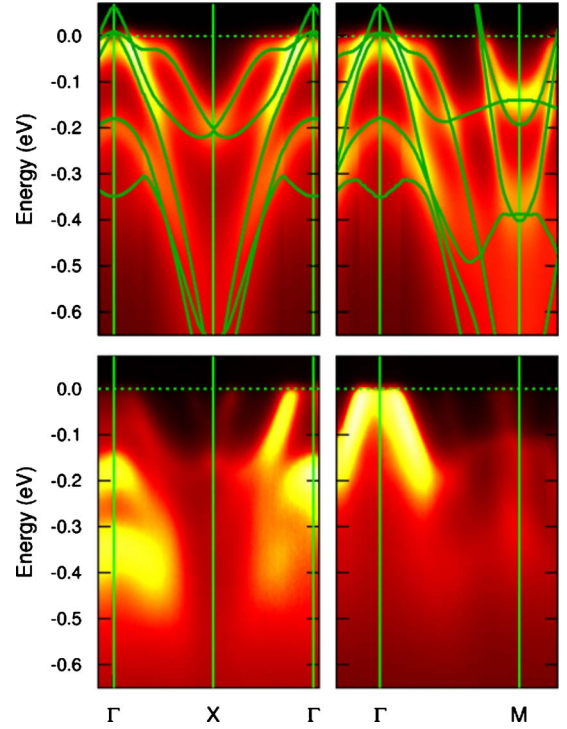

FIG. 3. (Color online) The **k**-resolved total spectral function $A(\mathbf{k}, \omega)$ of LaFePO along the Γ-X-Γ and Γ-M lines in the Brillouin zone is depicted as a contour plot. Upper panel: the LDA+DMFT spectral function. Lower panel: the corresponding experimental ARPES intensity map of Lu *et al.* (Ref. 6).

mass renormalization of a factor of 2 from optical conductivity data[7] and specific-heat measurements.[9]

We now calculate the **k**-resolved spectral function

$$A(\mathbf{k},\omega) = -\operatorname{Im}\frac{1}{\pi}\operatorname{Tr}[(\omega + \mu)\hat{I} - \hat{h}_{\mathbf{k}} - \hat{\Sigma}(\omega)]^{-1}. \qquad (2)$$

Here $\hat{h}_{\mathbf{k}} = \hat{H}_{LDA} - \hat{H}_{dc}$ is the 22×22 Hamiltonian matrix on a mesh of **k** points and μ is the self-consistently determined chemical potential. In Fig. 3 we compare our results with ARPES data of Lu *et al.*[6] Both theory and experiment show dispersive bands crossing the Fermi level near the Γ and M points. In addition, two bands can be seen at -0.2 eV and in the region from -0.3 to -0.4 eV near the Γ point. The calculated shape and size of the hole and electron pockets centered at the Γ and M points, respectively, are in good agreement with the ARPES, see Fig. 3 (lower panel), and de Haas–van Alphen[8] data.

The correlated band structure $\epsilon_{DMFT}(\mathbf{k})$ is also shown in Fig. 3 (upper panel). Near the Fermi energy, i.e., in the energy range from -0.2 eV to zero where quasiparticles are well defined [as expressed by a linear behavior of Re $\Sigma(\omega)$,

TABLE I. Effective mass renormalization m^*/m of quasiparticles in LaFePO for different orbitals of the Fe d shell from the LDA+DMFT calculation.

Orbitals	d_{xy}	$d_{yz,xz}$	$d_{3z^2-r^2}$	$d_{x^2-y^2}$
m^*/m	2.189	2.152	2.193	1.942

see Fig. 2], this dispersion is very well represented by the scaling relation $\epsilon_{DMFT}(\mathbf{k}) = \epsilon_{LDA}(\mathbf{k})/(m^*/m)$, with m^*/m taken as the computed mass enhancement from Table I.

The present results mean that the band structure in LaFePO is renormalized by the correlations and consists of the quasi-two-dimensional Fermi-surface sheets observed in the experiments. At the same time, there is no substantial spectral weight transfer from quasiparticle bands near the Fermi energy to Hubbard bands and the system is far away from metal-insulator transition. Such spectral function behavior does not allow to classify LaFePO either as *strongly* or *weakly* correlated material. According to classification proposed in Ref. 19, this material can be regarded as a *moderately* correlated metal such as $BaFe_2As_2$.[19]

In other iron pnictide materials the electron mass enhancement was also reported to be close to value of ≈ 2. For example, from the de Haas–van Alphen experiments $m^*/m = 1.13-3.41$ (Ref. 27) was found for $SrFe_2P_2$, isostructural analog of the superconducting compounds $Sr_{1-x}K_xFe_2As_2$ ($T_c = 37$ K). For the series of isostructural compounds $Ba(Fe_{1-x}Co_x)_2As_2$, $x = 0-0.3$ the authors of Ref. 28 evaluated $m^*/m = 2-4$ from the ARPES data. Also from the analysis of ARPES an electron mass renormalization by 2.7 was evaluated in $Ba_{0.6}K_{0.4}Fe_2As_2$ ($T_c = 37$ K) (Ref. 29) as comparing with the DFT-band structure. Further, the DFT-calculated plasma frequencies are by a factor of 1.5–2 larger than the experimental values,[30] showing the electron mass enhancement of the same strength for LaFePO, LaFeAsO, $SrFe_2As_2$, $BaFe_2As_2$, $K_{0.45}Ba_{0.55}Fe_2As_2$ ($T_c \approx 30$ K), and
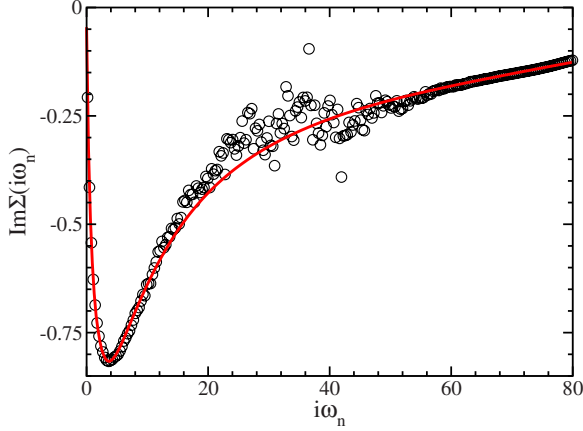
FIG. 4. (Color online) The imaginary part of the Fe d_{yz} self-energy $\Sigma(i\omega_n)$ calculated within LDA+DMFT (circles) is compared with the corresponding Padé approximant (curve).

LaO$_{0.9}$F$_{0.1}$FeAs ($T_c \approx 26$ K). From the reported data, it follows that the electronic correlation strength in the FeAs-based superconductors with the superconducting transition temperatures up to 37 K and their parent compounds is the same as in superconductor LaFePO with $T_c \approx 4$ K.[31] Thus, the strength of electronic correlations in the Fe-based superconductors seems to be not intrinsically connected with the superconducting transition temperature.

IV. CONCLUSION

By employing the LDA+DMFT method we have calculated the spectral functions and single-particle **k**-resolved spectrum of superconductor LaFePO for the first time. Very good agreement with the ARPES data was found. In the spectral functions we observed no substantial spectral weight transfer. The obtained effective electron mass enhancement values $m^*/m \approx 1.9 – 2.2$ are in good agreement with infrared and optical studies, de Haas–van Alphen, and specific-heat results. The electronic correlation strength in LaFePO with small value of superconducting temperature 4 K is similar to the other Fe-pnictide superconductors with the transition temperatures up to 37 K.
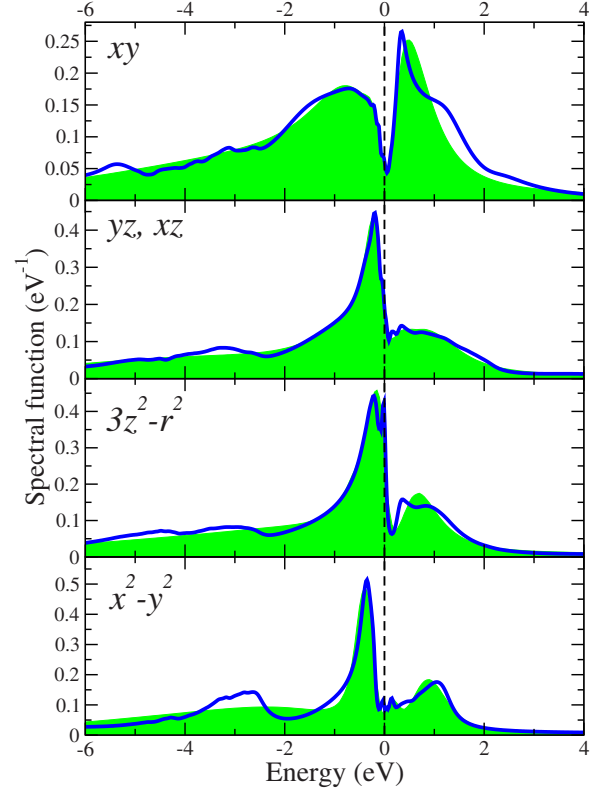
FIG. 5. (Color online) Orbitally resolved Fe $3d$ spectral functions of LaFePO from the maximum entropy method (green shaded areas) and the real-axis self-energy $\Sigma(\omega)$ obtained with the use of Padé approximation (blue curves).

APPENDIX: SELF-ENERGY ON THE REAL AXIS

In the DMFT method temperature (Matsubara) Green's-function formalism is used with arguments in the form of imaginary time τ or corresponding Matsubara imaginary energies $i\omega_n = i(2n+1)\pi/\beta$. In order to calculate a spectral function one needs to have self-energy as a function of real energy $\Sigma(\omega)$ that means to perform analytical continuation of the function $\Sigma(i\omega_n)$ to real axis. One of the usual algorithms for analytical continuation is Padé approximant,[26] and it was successfully used in earlier LDA+DMFT calculations where effective impurity problem was solved by iterative perturbation theory (IPT) method.[31] However, when impurity problem is solved by stochastic quantum Monte Carlo (QMC) method numerical noise appears in calculated $\Sigma(i\omega_n)$, see Fig. 4. Attempts to apply the Padé approximant method to such noisy data result in completely wrong widely oscillating real-axis function.

In order to solve this problem maximum entropy method[32] (MEM) was proposed. In this method spectral function $A(\omega)$ corresponding to imaginary time Green's

function $G(\tau)$ from QMC calculation is found as a best approximation to solution of the integral equation,

$$G(\tau) = -\int_{-\infty}^{\infty} d\omega \frac{e^{-\tau\omega}}{1 + e^{-\beta\omega}} A(\omega), \qquad (A1)$$

with the condition of maximization of effective entropy functional that gives a smooth spectral function. The resulting spectral function $A(\omega)$ is identified then with the **k**-integrated analog of Eq. (2) that gives equations for unknown self-energy $\Sigma(\omega)$. For many-orbital case that gives a set of equations with the corresponding number of unknown variables $\Sigma_i(\omega)$. Solution of such a set of equations can be a rather difficult problem. In addition to that the MEM method smears out all high-energy features in $A(\omega)$ due to the factor $e^{-\beta\omega}$ in the kernel of integral Eq. (A1).

In the present work we have used a modified version of the Padé approximant method. To make the analytical continuation procedure of the noisy self-energy $\Sigma(i\omega)$ numerically stable, we construct the approximant using only those frequency values where the self-energy is a smooth function. Practically that means to use a few first $i\omega_n$ at the lowest frequencies and the data at the large frequencies where $\Sigma(i\omega)$

approaches asymptotic behavior. In the result we obtain a smooth function that has correct analytical behavior at two limits: small energies $\omega \rightarrow 0$ and large energies where it obeys known asymptotic.

In Fig. 4 we compare the Fe d_{yz} self-energy $\Sigma(i\omega_n)$ obtained within Padé approximation with the corresponding numerical data from QMC solution of DMFT equations. The approximant has accurate derivatives in vicinity of zeroth Matsubara frequency, that guaranties correct analytical properties near the Fermi level and correct asymptotic behavior. At the same time it approximates the noisy region with a smooth curve.

In Fig. 5 the Fe $3d$ spectral functions obtained with Padé real-axis self-energy are compared with the MEM curves. The results for energies near the Fermi level are in very good agreement with each other. However, going to the higher and lower energies MEM curve very soon becomes smeared and nearly featureless while the curve obtained with Padé real-axis self-energy has much better resolved peaks and shoulders. For example, all the peaks in the energy region (−6, −2) eV are completely missed in MEM curve. This is due to exponential nature of the MEM kernel that suppresses all high-energy features.

---

[1] Y. Kamihara, H. Hiramatsu, M. Hirano, R. Kawamura, H. Yanagi, T. Kamiya, and H. Hosono, J. Am. Chem. Soc. **128**, 10012 (2006).

[2] Y. Kamihara, T. Watanabe, M. Hirano, and H. Hosono, J. Am. Chem. Soc. **130**, 3296 (2008); Z.-A. Ren, W. Lu, J. Yang, W. Yi, X.-L. Shen, C. Zheng, G.-C. Che, X.-L. Dong, L.-L. Sun, F. Zhou, and Z.-X. Zhao, Chin. Phys. Lett. **25**, 2215 (2008).

[3] Yu. A. Izyumov and E. Z. Kurmaev, Phys. Usp. **51**, 23 (2008).

[4] K. Kuroki, H. Usui, S. Onari, R. Arita, and H. Aoki, Phys. Rev. B **79**, 224511 (2009); J. D. Fletcher, A. Serafin, L. Malone, J. G. Analytis, J.-H. Chu, A. S. Erickson, I. R. Fisher, and A. Carrington, Phys. Rev. Lett. **102**, 147001 (2009).

[5] M. Yamashita, N. Nakata, Y. Senshu, S. Tonegawa, K. Ikada, K. Hashimoto, H. Sugawara, T. Shibauchi, and Y. Matsuda, Phys. Rev. B **80**, 220509(R) (2009).

[6] D. H. Lu, M. Yi, S.-K. Mo, A. S. Erickson, J. Analytis, J.-H. Chu, D. J. Singh, Z. Hussain, T. H. Geballe, I. R. Fisher, and Z.-X. Shen, Nature (London) **455**, 81 (2008); D. H. Lu, M. Yi, S.-K. Mo, J. G. Analytis, J.-H. Chu, A. S. Erickson, D. J. Singh, Z. Hussain, T. H. Geballe, I. R. Fisher, and Z.-X. Shen, Physica C **469**, 452 (2009).

[7] M. M. Qazilbash, J. J. Hamlin, R. E. Baumbach, L. Zhang, D. J. Singh, M. B. Maple, and D. N. Basov, Nat. Phys. **5**, 647 (2009).

[8] A. I. Coldea, J. D. Fletcher, A. Carrington, J. G. Analytis, A. F. Bangura, J.-H. Chu, A. S. Erickson, I. R. Fisher, N. E. Hussey, and R. D. McDonald, Phys. Rev. Lett. **101**, 216402 (2008).

[9] S. Suzuki, S. Miyasaka, S. Tajima, T. Kida, and M. Hagiwara, J. Phys. Soc. Jpn. **78**, 114712 (2009).

[10] S. Lebègue, Phys. Rev. B **75**, 035110 (2007).

[11] W. L. Yang, A. P. Sorini, C-C. Chen, B. Moritz, W.-S. Lee, F. Vernay, P. Olalde-Velasco, J. D. Denlinger, B. Delley, J.-H. Chu, J. G. Analytis, I. R. Fisher, Z. A. Ren, J. Yang, W. Lu, Z. X.

Zhao, J. van den Brink, Z. Hussain, Z.-X. Shen, and T. P. Devereaux, Phys. Rev. B **80**, 014508 (2009).

[12] V. Vildosola, L. Pourovskii, R. Arita, S. Biermann, and A. Georges, Phys. Rev. B **78**, 064518 (2008).

[13] R. Che, R. Xiao, C. Liang, H. Yang, C. Ma, H. Shi, and J. Li, Phys. Rev. B **77**, 184518 (2008).

[14] Y. Kamihara, M. Hirano, H. Yanagi, T. Kamiya, Y. Saitoh, E. Ikenaga, K. Kobayashi, and H. Hosono, Phys. Rev. B **77**, 214515 (2008).

[15] G. Kotliar, S. Y. Savrasov, K. Haule, V. S. Oudovenko, O. Parcollet, and C. A. Marianetti, Rev. Mod. Phys. **78**, 865 (2006); K. Held, I. A. Nekrasov, G. Keller, V. Eyert, N. Blümer, A. K. McMahan, R. T. Scalettar, Th. Pruschke, V. I. Anisimov, and D. Vollhardt, Psi-k Newsletter **56**, 65 (2003); reprinted in Phys. Status Solidi B **243**, 2599 (2006).

[16] K. Haule, J. H. Shim, and G. Kotliar, Phys. Rev. Lett. **100**, 226402 (2008).

[17] M. Aichhorn, L. Pourovskii, V. Vildosola, M. Ferrero, O. Parcollet, T. Miyake, A. Georges, and S. Biermann, Phys. Rev. B **80**, 085101 (2009).

[18] V. I. Anisimov, Dm. M. Korotin, M. A. Korotin, A. V. Kozhevnikov, J. Kuneš, A. O. Shorikov, S. L. Skornyakov, and S. V. Streltsov, J. Phys.: Condens. Matter **21**, 075602 (2009); A. O. Shorikov, M. A. Korotin, S. V. Streltsov, S. L. Skornyakov, Dm. M. Korotin, and V. I. Anisimov, Sov. Phys. JETP **108**, 121 (2009); V. I. Anisimov, E. Z. Kurmaev, A. Moewesb, and I. A. Izyumov, Physica C **469**, 442 (2009).

[19] S. L. Skornyakov, A. V. Efremov, N. A. Skorikov, M. A. Korotin, Yu. A. Izyumov, V. I. Anisimov, A. V. Kozhevnikov, and D. Vollhardt, Phys. Rev. B **80**, 092501 (2009).

[20] V. I. Anisimov, D. E. Kondakov, A. V. Kozhevnikov, I. A. Nekrasov, Z. V. Pchelkina, J. W. Allen, S.-K. Mo, H.-D. Kim, P.

Metcalf, S. Suga, A. Sekiyama, G. Keller, I. Leonov, X. Ren, and D. Vollhardt, Phys. Rev. B **71**, 125119 (2005).

[21] B. I. Zimmer, W. Jeitschko, J. H. Albering, R. Glaum, and M. Reehuis, J. Alloys Compd. **229**, 238 (1995).

[22] http://elk.sourceforge.net/

[23] P. Werner, A. Comanac, L. de' Medici, M. Troyer, and A. J. Millis, Phys. Rev. Lett. **97**, 076405 (2006).

[24] A. I. Liechtenstein, V. I. Anisimov, and J. Zaanen, Phys. Rev. B **52**, R5467 (1995).

[25] Dm. Korotin, A. V. Kozhevnikov, S. L. Skornyakov, I. Leonov, N. Binggeli, V. I. Anisimov, and G. Trimarchi, Eur. Phys. J. B **65**, 91 (2008).

[26] H. J. Vidberg and J. W. Serene, J. Low Temp. Phys. **29**, 179 (1977).

[27] J. G. Analytis, C. M. J. Andrew, A. I. Coldea, A. McCollam, J.-H. Chu, R. D. McDonald, I. R. Fisher, and A. Carrington, Phys. Rev. Lett. **103**, 076401 (2009).

[28] V. Brouet, M. Marsi, B. Mansart, A. Nicolaou, A. Taleb-Ibrahimi, P. Le Fèvre, F. Bertran, F. Rullier-Albenque, A. Forget, and D. Colson, Phys. Rev. B **80**, 165115 (2009).

[29] M. Yi, D. H. Lu, J. G. Analytis, J.-H. Chu, S.-K. Mo, R.-H. He, R. G. Moore, X. J. Zhou, G. F. Chen, J. L. Luo, N. L. Wang, Z. Hussain, D. J. Singh, I. R. Fisher, and Z.-X. Shen, Phys. Rev. B **80**, 024515 (2009).

[30] S. Drechsler, H. Rosner, M. Grobosch, G. Behr, F. Roth, G. Fuchs, K. Koepernik, R. Schuster, J. Malek, S. Elgazzar, M. Rotter, D. Johrendt, H-H. Klauss, B. Büchner, and M. Knupfer, arXiv:0904.0827 (unpublished).

[31] V. I. Anisimov, A. I. Poteryaev, M. A. Korotin, A. O. Anokhin, and G. Kotliar, J. Phys.: Condens. Matter **9**, 7359 (1997).

[32] M. Jarrell and J. E. Gubernatis, Phys. Rep. **269**, 133 (1996).